

Molecular photoionization in the linear algebraic approach:  $H_2$ ,  $N_2$ ,  $NO$ , and  $CO_2$ 

L. A. Collins and B. I. Schneider

*Theoretical Division, Los Alamos National Laboratory, Los Alamos, New Mexico 87545*

(Received 20 October 1983)

We extend the linear algebraic method to the calculation of molecular photoionization cross sections. The formulation is primarily developed in the fixed-nuclei, Hartree-Fock, and frozen-core approximations, although correlation effects in the scattering solution are introduced through an effective optical potential. The single-center expansion and close-coupling approximations are invoked to give converged scattering solutions. Cross sections and asymmetry parameters are reported for photoionization from the ground state of  $H_2$ ,  $N_2$ ,  $NO$ , and  $CO_2$ . We obtain very good agreement with the Schwinger variational results of McKoy and co-workers for all molecular systems. For  $NO$  and  $CO_2$ , we find substantial disagreements with the Stieltjes calculations for some symmetries.

## I. INTRODUCTION

The understanding and analysis of a wide variety of physical and chemical phenomena depend on a knowledge of molecular photoionization.<sup>1</sup> Photoionization processes play vital roles in the construction of models to represent planetary atmospheres<sup>2(a)</sup> and astrophysical objects,<sup>2(b)</sup> such as comets and circumstellar clouds. In addition, the orientation of a molecule absorbed on a surface can be determined from the angular distribution of the ejected electron.<sup>3</sup> Also, with the advent of the tunable synchrotron sources,<sup>4</sup> detailed investigations of the energy and angular dependence of the photoionization cross section are now possible. Therefore, the development of reliable theoretical models for efficiently calculating photoionization quantities has become an important endeavor for collision physicists.

The calculation of photoionization cross sections can be reduced to the evaluation of a multipole matrix element, usually the dipole. This matrix element, in turn, is related to the bound-state wave functions of the target and residual ionic molecules and to the continuum solution for the ejected electron. The following three methods have been the most extensively applied to the calculation of photoionization quantities: (1) the Stieltjes-Tchebycheff moment theory (STMT),<sup>5-8</sup> (2) the Schwinger variational (SV) method,<sup>9-12</sup> and (3) the continuum multiple scattering method (CMSM).<sup>13</sup> In addition, calculations have been performed using many-body perturbation theory (MBPT),<sup>14</sup> a time-dependent, local density approximation (TDLDA),<sup>15</sup> the random-phase approximation with exchange (RPAE),<sup>15(b)</sup> and various iterative and noniterative continuum methods.<sup>16</sup> The STMT approach represents the bound and continuum wave functions on an  $L^2$  basis, while the SV method and CMSM employ different prescriptions for determining these two wave functions. The bound-state wave functions are still determined by  $L^2$  techniques while the continuum wave function is determined from a numerical solution of the electron-ion Schrödinger equation.

In this paper, we extend our linear algebraic (LA)

method for obtaining continuum electron-molecule solutions to the realm of photoionization. The LA method has been successfully applied at the static-exchange (SE) or continuum Hartree-Fock (HF) level to a plethora of molecular systems.<sup>17</sup> In addition, we have introduced an effective optical potential into the Schrödinger equation for elastic scattering in order to treat correlation effects.<sup>18</sup> The results for  $e-H_2^+$ ,  $-H_2$ , and  $-N_2$  collisions are in quite good agreement with those of other theoretical approaches and with experiment. We have also applied the LA technique to the electronic excitation of atoms and of the  $H_2^+$  molecule.<sup>19</sup> The success of the method in handling such a wide variety of electron-molecule scattering processes led us to believe that it would be equally well suited for photoionization.

In our formulation of photoionization, we treat the bound and continuum wave functions independently. The bound-state functions are calculated with a standard molecular structure package while the continuum solution is determined by the LA method. The separate functions are then combined in the dipole matrix element to yield a photoionization cross section. Our basic application is at the Hartree-Fock level for the bound and continuum wave functions. In addition, we make the frozen-core (FC) approximation by which the neutral molecular orbitals are used to represent those of the ion. For photoionization, the frozen-core Hartree-Fock (FCHF) scheme has been shown to give a reasonably accurate representation of the cross section and asymmetry parameter.<sup>5-16</sup> We go beyond this approximation by using an effective optical potential to introduce correlation effects into the elastic scattering solution. This addition allows us to obtain autoionization structure which is absent from the FCHF approach.

We treat photoionization of ground state  $H_2$ ,  $N_2$ ,  $NO$ , and  $CO_2$ . Our purpose in selecting these systems is twofold. First, we wish to test the accuracy of the LA approach for photoionization. To this end, we select systems such as  $H_2$  and  $N_2$  that have received extensive theoretical attention. Second, we wish to resolve some of the differences between the Stieltjes and Schwinger results

for NO and CO<sub>2</sub>.

The remainder of the paper is divided into three sections. In Sec. II we briefly review the formalism for molecular photoionization, while in Sec. III we present the results of our LA calculation. Finally, we summarize our findings and draw conclusions in Sec. IV.

## II. METHODS

In this section, we develop the formalism necessary to treat the process of molecular photoionization. Since the details of this formulation are presented elsewhere, we premit all but the most important aspects of the formal development. In general, we follow closely the treatment of Tully, Berry, and Dalton.<sup>20</sup> Since their formulation is restricted to photoionization from closed-shell molecules, we have made some modifications in their formulas to encompass the more general case of open-shell targets. We neglect rotational and vibrational motion of the molecule and thus confine our treatment to the fixed-nuclei (FN) approximation.<sup>21</sup> In addition, we consider ionization only out of the ground state of the target molecule, although we shall introduce virtual electronic excitations through an effective optical potential.

### A. General formulation

We consider the following photoionization process:



The initial state is characterized by the  $N$ -electron molecular wave function  $\Phi_{\Lambda_i S_i}(1, \dots, N)$  of the neutral, target molecule, while the final state is composed of an antisymmetric linear combination of product wave functions  $\Psi_{\Gamma lm}(1, \dots, N)$  representing the residual ion core  $\Phi_{\Lambda_c S_c}(1, \dots, N-1)$  and the scattered electron  $\Psi_{lms}(N)$ . The quantum numbers  $\Lambda$  and  $S$  refer to the projection of the total orbital angular momentum of the molecular electrons onto the internuclear axis and to the spin state of the molecule, respectively. Similarly, the parameters  $m$  and  $s$  are the analogs of  $\Lambda$  and  $S$ , but refer to the electron-plus-molecular-ion system. The quantity  $l$  gives the value of the orbital angular momentum of the outgoing, ionized electron and labels a particular linearly independent scattering solution. Finally, we introduce the customary abbreviation  $\Gamma$  for the quantum numbers describing the molecular ion and the spin state of the electron [ $\Gamma = (\Lambda_c S_c s)$ ]. In the dipole approximation to the radiation field, the observables associated with the photoionization process, such as the cross section and asymmetry parameter, are related to a dipole matrix element of the form

$$\langle \Phi_{\Lambda_i S_i} | D | A(\Phi_{\Lambda_c S_c} \Psi_{lms}) \rangle, \quad (2)$$

where  $D$  ( $A$ ) is the dipole (antisymmetry) operator.

In a more comprehensive form, we write the differential photoionization cross section for an ensemble of arbitrarily oriented molecules as<sup>20</sup>

$$\sigma_{\Gamma}(\Omega) = A_{00} + A_{20} P_2^0(\cos\theta), \quad (3)$$

where  $P_2^0$  is an associated Legendre polynomial of order 2,

and  $\theta$  is the angle between the direction of polarization of the light and the momentum of the outgoing electron. This formulation is also referred to as the integrated target angular distribution (ITAD). The  $A$  coefficients have the following form:

$$A_{\xi 0} = \Delta \sum_{lm, \lambda u} (\cos\gamma_{l\lambda} F_{lm, \lambda u} - \sin\gamma_{l\lambda} G_{lm, \lambda u}) C_{\xi}(l\lambda | mu), \quad (4)$$

where

$$\gamma_{l\lambda} = \eta_l - \eta_{\lambda} + (\lambda - l)\pi/2, \quad (5)$$

$$F_{lm, \lambda u} = \text{Red}_{lm} \text{Red}_{\lambda u} + \text{Imd}_{lm} \text{Imd}_{\lambda u}, \quad (6a)$$

$$G_{lm, \lambda u} = \text{Imd}_{lm} \text{Red}_{\lambda u} - \text{Red}_{lm} \text{Imd}_{\lambda u}, \quad (6b)$$

$$C_{\xi}(l\lambda | mu) = (-1)^{m_j} \frac{[(2l+1)(2\lambda+1)]^{1/2}}{4\pi(2\xi+1)} \\ \times C(11\xi | 0,0) C(\lambda l\xi | 0,0) \\ \times C(\lambda l\xi | u, -m) C(11\xi | -m - m_j, u + m_j), \quad (7)$$

$$d_{lm} = \left[ \prod_k \int dr_k \psi_{\Gamma lm} r_k Y_{1m''} \Phi_{\Lambda_i S_i} \right]_{m''=m-m_j}, \quad (8)$$

$$\Delta = \frac{4\pi^2 \alpha \hbar \omega}{3},$$

with  $\alpha$  denoting the fine-structure constant,  $\hbar\omega$  the photon energy,  $m_j = \Lambda_c - \Lambda_i$ ,  $\eta_l$  the Coulomb phase shift, and  $C(l, l_2 l_3 | m, m_2)$  a Clebsch-Gordan coefficient. The difference in the Coulomb phases ( $\eta_l - \eta_{\lambda}$ ) is calculated by the geometric formula of Dill.<sup>22</sup> The integration in Eq. (8) is assumed to go over the configuration space of all electrons.

By integrating Eq. (3) over all solid angles, we obtain an expression for the photoionization cross section

$$\sigma_{\Gamma} = 4\pi A_{00}. \quad (9)$$

The asymmetry parameter  $\beta$  is also given in terms of the  $A$  coefficients by

$$\beta = A_{20}/A_{00}. \quad (10)$$

For the case of  $\xi = 0$ , we can simplify much of the Racah algebra in Eqs. (3)–(7) and derive a rather compact form for the photoionization cross section

$$\sigma_{\Gamma} = \frac{\Delta}{3} \sum_{l,m} |d_{lm}|^2. \quad (11)$$

The cross section represented by Eq. (11) is characterized by particular symmetries of the neutral and ionic molecules. The total photoionization cross section  $\sigma_{\text{ph}}$  is found by summing over the final states of the core ion and averaging over the initial states of the target molecule.

## B. Approximations

We introduce several approximations to the above formulation which simplify the analysis and facilitate the computational aspects without seriously degrading the quality of the results.

### 1. Bound-state orbitals—frozen core

We calculate the neutral and ionic molecular bound-state wave functions at the HF level using standard molecular structure programs.<sup>23(a)</sup> The bound functions can then be represented as a single Slater determinant of the form

$$\Phi_{AS}(\vec{r}_1, \dots, \vec{r}_N) = |\phi_1(1)\bar{\phi}_1(2) \cdots \phi_n(N-1)\bar{\phi}_n(N)| \quad (12)$$

for closed-shell systems, where  $n$  is the number of *occupied orbitals* and  $\phi_i(j)$  represents a spin orbital. For open-shell molecules, we must usually take a linear combination of determinants with partially filled orbitals in order to construct a system wave function with the proper orbital and spin angular momenta symmetries.

We introduce the *frozen-core approximation* by which the HF orbitals of the neutral, target molecule are used to represent those of the residual ion core. This substitution leads to a considerable simplification in the form of the dipole matrix elements  $d_{lm}$ . The  $d_{lm}$  quantities now depend only on the ionized and scattering *orbitals* and have the general form

$$d_{lm} = N_0^{1/2} \int d\vec{r} \psi_l^m(\vec{r}) r Y_{lm}(\hat{r}) \phi_j^{m_j}(\vec{r}), \quad (13)$$

where  $\phi_j^{m_j}$  is the spatial HF orbital of symmetry  $m_j$  ( $=\Lambda_c - \Lambda_i$ ) of the neutral molecule from which an electron is ejected,  $\psi_l^m(\vec{r})$  is the scattering orbital, and  $N_0$  is the occupation number of the ionized orbital ( $=1$  or  $2$ ). Setting  $N_0=2$ , we recover the closed-shell formulas of Tully *et al.*; the choice of  $N_0=1$  restricts us to a single-occupied orbital outside a closed-shell core. For other cases, we must determine  $N_0$  by constructing the proper combination of determinants to give the correct spin and angular symmetry of the system. We have dropped the subscript involving spin and assumed that it has been properly treated in the bound-state and scattering calculations.

We evaluate Eq. (13), which is the key to constructing the photoionization parameters, by performing a single-center expansion of the molecular and scattering orbitals

$$\psi_l^m(\vec{r}) = r^{-1} \sum_{l'} \psi_{l'}^m(r) Y_{l'm}(\hat{r}), \quad (14a)$$

$$\phi_j^{m_j}(\vec{r}) = r^{-1} \sum_{l_j} \phi_{l_j}^{m_j}(r) Y_{l_j m_j}(\hat{r}). \quad (14b)$$

The radial coefficients for the scattering orbital  $\psi_{l'}^m$  are determined by solving a set of radial coupled integro-differential equations as described in Sec. IIB2 and in Refs. 17 and 18. Since the bound molecular orbitals are expressed in terms of Cartesian Gaussians, the radial expansion coefficients can be determined from a set of

analytical recursion relations in terms of modified spherical Bessel and associated Legendre functions. Substituting Eqs. (14) into Eq. (13), we find

$$d_{lm} = N_0^{1/2} \sum_{l', l_j} X(l_j l' | m_j m'' m) D(l' l l_j), \quad (15)$$

where

$$D(l' l l_j) \equiv \int \psi_{l'}^m(r) r \phi_{l_j}^{m_j}(r) dr, \quad (15')$$

$$X(l_1 l_2 l_3 | m_1 m_2 m_3) \equiv \left[ \frac{3(2l_1 + 1)}{4\pi(2l_3 + 1)} \right]^{1/2} \times C(l_1 l_2 l_3 | m_1 m_2 m_3) \times C(l_1 l_2 l_3 | 000), \quad (15'')$$

$m_j = \Lambda_i - \Lambda_c$ . We reiterate that  $l$  labels a particular linearly independent solution of the scattering wave function while  $l'$  labels a component of the single-center expansion. The scattering wave function satisfies  $S$ -matrix boundary conditions, making  $d_{lm}$  a complex quantity. We usually choose to work with real functions in the scattering calculations and thus with  $K$ -matrix boundary conditions. The two wave functions  $\psi_S$  and  $\psi_K$ , with  $S$ - and  $K$ -matrix boundary conditions, respectively, are related by<sup>16(c)</sup>

$$\text{Im} \psi_S = 2 \psi_K (\underline{1} + \underline{K} \underline{K})^{-1}, \quad (16a)$$

$$\text{Re} \psi_S = (\text{Im} \psi_K) \underline{K}, \quad (16b)$$

where  $\underline{K}$  is the reactance matrix.

### 2. Continuum solutions

The Schrödinger equation which describes the collision of an electron with an  $N$ -electron target molecule has the following form:

$$H |\Psi\rangle = E |\Psi\rangle, \quad (17)$$

where

$$H = H_T + T_e + V_{en} + \sum_{i=1}^N g_{ie}, \quad (18a)$$

$H_T$  denoting the Hamiltonian of the target molecule,

$$T_e = -\frac{1}{2} \nabla_e^2, \quad (18b)$$

$$V_{en} = - \sum_{\alpha} Z_{\alpha} | \vec{r}_e - \vec{r}_{\alpha} |^{-1}, \quad (18c)$$

and

$$g_{ie} = | \vec{r}_i - \vec{r}_e |^{-1} \quad (18d)$$

with  $\vec{r}_e$  ( $\vec{r}_i$ ) the position of the scattering (target) electron and  $Z_{\alpha}$  ( $r_{\alpha}$ ) the charge (position) of nucleus  $\alpha$ . In order to solve Eq. (17) we divide configuration space into two regions with the boundary at  $r=a$ . In the outer region, where nonlocal effects are negligible and the potential is local and usually multipolar in form, we employ standard coupled-channel propagation procedures to integrate the

solution from  $r = a$  into the asymptotic region.<sup>23(b)</sup>

In the inner region, where exchange and correlation effects are important, we expand the total system wave function  $|\psi\rangle$  as follows:

$$|\psi\rangle = \sum_{c=1}^m A(\phi_c(1, \dots, N)\psi_c(N+1)) + \sum_q C_q \psi_q(1, \dots, N+1), \quad (19)$$

where  $\phi_c$  is an  $N$ -electron target molecular-ion wave function and  $\psi_c$  is the scattering wave function. The set of "correlation" functions  $\{\psi_q\}$  is added for completeness and can be selected as pseudostates or electronically excited states of the target-plus-electron system. By introducing projection operators of the form

$$P|\chi\rangle = \sum_c A(\phi_c(1, \dots, N)\chi_c(N+1)), \quad (20a)$$

$$Q|\chi\rangle = \sum_q d_q \psi_q(1, \dots, N+1), \quad (20b)$$

$$P+Q=I,$$

with  $|\chi\rangle$  an arbitrary  $(N+1)$ -electron function, we can partition the Schrödinger equation (17) into the standard Feshbach form<sup>24</sup>

$$(H_{PP} + V_{\text{opt}} - E)P|\psi\rangle = 0, \quad (21a)$$

$$V_{\text{opt}} = H_{PQ}(E - H_{QQ})^{-1}H_{QP}, \quad (21b)$$

$$(E - H_{QQ})Q|\psi\rangle = H_{QP}P|\psi\rangle, \quad (21c)$$

where  $H_{XY} \equiv XHY$  with  $X, Y = P$  or  $Q$ .

In this study, we will confine our discussion to the elastic scattering solution. Thus, we truncate the expansion in Eqs. (19) and (20a) at a single term ( $c=1$ ), the ground state of the target system, and choose  $\psi_q$  to represent the effects of virtual excitations to closed excited electronic states.

*a. Static exchange or continuum Hartree-Fock.* In the SE approximation, we further restrict the form of the total system wave function in Eq. (19) by neglecting the correlation functions in the expansion ( $C_q=0$ ). The system wave function then becomes a simple antisymmetric product of the continuum and ground-state wave functions. If we substitute the expression for  $|\psi\rangle$  into Eq. (21), multiply through by the ground-state molecular wave function, and integrate over the coordinates of the bound electrons, we obtain the standard SE equation for the scattering orbital<sup>10</sup>

$$\left\{ f + \sum_{i=1}^n (2a_i J_i - b_i K_i) - \epsilon \right\} \psi_i^m = \sum_{k=1}^n \lambda_k \phi_k, \quad (22)$$

where

$$f = T_e + V_{en},$$

$$J_i(1)\chi_j(1) = \langle \chi_i(2) | g_{12} | \chi_j(2) \rangle \chi_j(1), \quad (23a)$$

$$K_i(2)\chi_j(1) = \langle \chi_i(2) | g_{12} | \chi_j(2) \rangle \chi_i(1), \quad (23b)$$

where  $J_i$  and  $K_i$  are the standard Coulomb and exchange

operators with  $\chi_\alpha$  either  $\phi_\alpha$  or  $\psi_i^m$ , and  $\epsilon$  is the energy of the outgoing electron in hartrees. The summation in Eq. (22) runs over all occupied orbitals of the molecular ion; the coefficients  $a_i$  and  $b_i$  are selected according to the spin state and symmetry of the scattering function desired. For example, for doublet scattering from a closed-shell molecule,  $a = 1$  and  $b = 1$  for all occupied orbitals. We include the values of  $a$  and  $b$  for each system and symmetry in tables in Sec. IV; a more complete compilation can be found in Rose and McKoy.<sup>25</sup>

The term on the right-hand side of Eq. (22) is added in order to force the orthogonality of the scattering and bound-state orbitals of the same symmetry. For a closed-shell molecule represented by a HF wave function, the scattering solution is formally orthogonal to the bound orbitals since they satisfy the same Schrödinger equation. However, in the FC approximation this is no longer the case since the neutral molecular orbitals are used to construct the ionic molecular wave function. We must therefore guarantee the orthogonality by introducing *a posteriori* the Lagrange undetermined multipliers (LUM)  $\lambda_k$ .

*b. Effective optical potential.* As a first step for going beyond the SE approximation, we consider the effects on the elastic scattering solution of introducing correlation effects through an effective optical potential  $V_{\text{opt}}$  [Eq. (21b)]. For photoionization processes, the introduction of correlation into the scattering orbital allows us to describe autoionization features which are not present at the SE level.

The partitioning introduced into the Schrödinger equation (17) is strictly formal. We take advantage of the form of Eq. (21a) by making the additional approximation of evaluating the optical potential on an  $L^2$  basis. Since both the continuum and bound-state parts of  $V_{\text{opt}}$  are represented by an  $L^2$  basis, the evaluation of the optical potential can be divorced from the scattering calculation. We calculate  $V_{\text{opt}}$  by standard configuration-interaction (CI) bound-state methods<sup>23</sup> and introduce the resulting expression into the scattering equation. Since such a prescription represents a "reconciliation" or union between the  $L^2$  and numerical close-coupling approaches, we might term these methods syncretic.

As in the SE case, we derive an equation for the scattering orbital  $\psi_i^m$  by multiplying Eq. (21) by the ground-state molecular wave function and by integrating over the coordinates of the bound electrons. The resulting equation has the form

$$\left\{ f + \sum_i 2a_i J_i + U_c(\vec{r}_j \vec{r}_j') - \epsilon \right\} \psi_i^m = \sum_k \lambda_k \phi_k, \quad (24)$$

where  $U_c$  contains both the exchange and the optical-potential contributions. The Lagrange undetermined multipliers are introduced to force orthogonality of the continuum orbital to all bound orbitals of the same symmetry. For a more thorough discussion of the effective optical potential method, we refer the reader to an earlier set of publications.<sup>18</sup>

One further point is in order. The total system wave function is given by

$$|\psi\rangle = P|\psi\rangle + Q|\psi\rangle,$$

and it is this expression which should be used in the evaluation of the dipole matrix element in Eq. (8). However, as a first approximation, we shall only use the  $P$  space or scattering part of the system wave function as calculated from Eq. (21a) or Eq. (24). Retention of the scattering part will guarantee a reasonable representation of the autoionization features; the absolute magnitude of the photoionization may be in some error due to the neglect of the  $Q|\psi\rangle$  component.<sup>26</sup>

*c. Method of solution.* In this final subsection, we describe the methods we employ to solve Eqs. (22) and (24). Once again, we present only a cursory description since the details are presented in other publications.<sup>17-19</sup> We first convert Eq. (22) or Eq. (24) to a set of coupled, radial integro-differential equations by expanding the bound and continuum orbitals in terms of spherical harmonics [Eq. (14)] and by integrating over all angular coordinates. This set of scattering equations is further transformed to a set of coupled integral equations by means of the Coulomb Green's functions. Finally, by introducing a discrete quadrature for the evaluation of the integrals, we obtain a set of LA equations. We then employ standard linear systems routines to solve the LA equations for the radial scattering orbitals. We emphasize that the LA equations are solved in the region  $r \leq a$  in which nonlocal effects are important. For  $r > a$ , where the potential is local, we extend the solution into the asymptotic region by a standard propagation scheme.<sup>27</sup> We then match the solution to a linear combination of regular and irregular Coulomb functions in order to obtain the reactance or  $K$  matrix.

We treat the exchange or exchange-plus-optical-potential terms in a separable approximation.<sup>17,28</sup> In other words, we represent the general exchange kernel in terms of a complete set of basis functions as

$$U_c(\vec{r}, \vec{r}', \epsilon) = \sum_{\alpha} \chi^{\alpha}(\vec{r}, \epsilon) \Lambda_{\alpha}(\epsilon) \chi^{\alpha}(\vec{r}', \epsilon), \quad (25)$$

where

$$\Lambda_{\alpha}(\epsilon) = \int \int \chi^{\alpha}(\vec{r}, \epsilon)^{\dagger} U(\vec{r}, \vec{r}', \epsilon) \chi^{\alpha}(\vec{r}', \epsilon) d\vec{r} d\vec{r}'.$$

The general form of Eq. (25) involves a double summation over the separable basis. We have shown, however, that for the case of electronically elastic scattering that this term can be placed in diagonal form by a simple unitary transformation.<sup>17,18</sup> The complete set of functions that form the separable basis is usually constructed from a set of occupied and virtual molecular orbitals of the symmetry of the scattering orbital.<sup>17</sup>

We make one additional approximation to the solution of the coupled radial equations. The sums in Eqs. (14), which represent single-center expansions, run over an infinite number of terms. We therefore enforce the close-coupling (CC) approximation by which these sums are truncated at a finite upper limit. In order to guarantee accurate solutions, we must assiduously and systematically increase the limits until the various photoionization parameters converge to within a given tolerance. With the proper care, single-center expansions can be made to give highly accurate solutions of the continuum electron-molecule Schrödinger equation.<sup>29</sup> Its efficacy and effi-

ciency have been demonstrated by numerous groups for a diverse set of molecular targets.<sup>9-12,16-19,28-30</sup>

### III. RESULTS

Before proceeding to a discussion of our results for  $H_2$ ,  $N_2$ ,  $NO$ , and  $CO_2$ , we review the salient features of our photoionization calculations:

- (1) Dipole length-convention.
- (2) Bound orbitals: Hartree-Fock and frozen-core approximations.
- (3) Continuum orbitals: static-exchange or effective-optical-potential approximations.
- (4) Single-center expansion and close-coupling approximation.
- (5) Fixed-nuclei approximation.

We apply the more standard label FCHF for the frozen-core, static-exchange case.

We also present the following summary of the nomenclature used throughout this section:

- (1)  $n_c$  denotes the number of terms retained in the expansion of the continuum orbital [Eq. (14a)] in the solution of the coupled scattering equations (22) and (24);
- (2)  $n_e$  is the same as  $n_c$  except for the exchange term;
- (3)  $n_f$  is the number of separable basis functions retained in the representation of the exchange or optical-potential terms [Eq. (25)];
- (4)  $r_a$  is the radius of the  $R$ -matrix boundary ( $=a$ );
- (5)  $r_m$  is the asymptotic matching radius; and
- (6)  $n_p$  is the total number of points in the Gauss-Legendre mesh for the quadrature of the integrals in the continuum Schrödinger equation.

The maximum value of  $l$  retained in a particular expansion is given by

$$l_{\max} = \Delta l(n-1) + l_0, \quad (26)$$

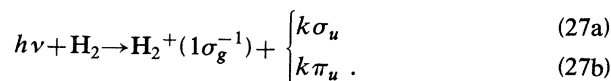
where  $n = n_c$  or  $n_e$ ,  $\Delta l = 1$  (2) for a polar (homonuclear) molecule, and  $l_0$  is the initial value of  $l$  for a given scattering symmetry. For example, for  $\sigma_u$  scattering from  $N_2^+(3\sigma_g^{-1})$  with  $n_c = 10$ , we have  $l_0 = 1$  and  $l_{\max} = 19$ . The static potential is also expanded in terms of spherical harmonics with all values retained up to  $2l_{\max}$ . Owing to the nature of the separable potential, the sum over the expansion coefficients of the bound orbitals is performed implicitly and is effectively infinite.<sup>17</sup> The integrals in the scattering equations are evaluated with a Gauss-Legendre quadrature. Usually, the region from  $r=0$  to  $r=r_a$  is divided into a set of subregions, each with a different number of points. We designate this regional division by  $[n_1, n_2, n_3 | r_1, r_2]$ . The first subregion extends from  $r=0$  to  $r=r_1$  and contains  $n_1$  Gauss-Legendre points, the second subregion from  $r=r_1$  to  $r=r_2$  with  $n_2$  points, and the third from  $r=r_2$  to  $r=r_a$  with  $n_3$  points. The choice of meshes employed in this study guarantees a convergence of 5% or better. Since for the lower partial waves which exhibit oscillatory behavior we must include a minimum number of points for each half-wavelength, the

number of mesh points must be increased as we move to higher energies. Finally, in the evaluation of the photoionization quantities, we choose the bound and continuum orbital expansions to have the same limit as the continuum expansion in the scattering solution.

We generally choose  $r_m = r_a$ . At first, this choice may seem rather restrictive. However, since the long-range ( $r \geq 10a_0$ ) Coulomb potential dominates even the dipole term, we can safely match to Coulomb functions at moderately small radii. To see this more clearly, we note that the ratio of the Coulomb to dipole term is given by  $qr/D$ , where  $q$  is the residual ion charge and  $D$  is the ionic dipole moment. For  $\text{NO}^+$ , the dipole moment is 0.6 a.u., implying that the Coulomb term is already an order of magnitude larger at  $r = 10a_0$ . We have performed several tests for  $r_m = 1.5r_a$  and  $r_m = 2r_a$  in order to check this assumption and found sensitivities of less than 5% to the choice of matching radius. With these conventions in hand, we are now ready to proceed to a discussion of the photoionization results.

### A. Photoionization of $\text{H}_2$

As a first application of the LA approach to photoionization, we chose  $\text{H}_2$ . We consider the following process for ionization of the  $1\Sigma_g^+$  ground-state molecule:



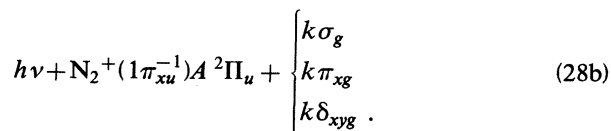
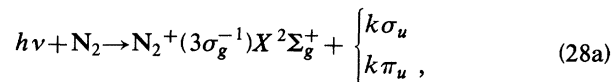
In Table I, we present a description of the two Gaussian bases employed to construct the bound and separable exchange orbitals. Basis 1 is similar to one employed by Lucchese and McKoy to study  $e\text{-H}_2^+$  collisions,<sup>31</sup> while basis 2 is patterned after that suggested by O'Neil and Reinhardt.<sup>32</sup> Basis 2 has a slightly more diffuse character than basis 1. The diffuse functions at the c.m. are included primarily to give a better representation of the separable orbitals. In addition, we calculated the photoionization cross section using the Slater-type orbital (STO) bases of Fraga and Ransil (FR)<sup>33</sup> and of Cade and Wahl (CW).<sup>34</sup> All four wave functions produce total Hartree-Fock energies and quadrupole moments ( $Q$ ) for  $\text{H}_2$  in quite good agreement. The total energies ( $Q$ ) are as follows for the ground-state wave functions produced by bases 1, 2, FR,

and CW:  $-1.13310$  (0.50),  $-1.13326$  (0.49),  $-1.133$  (0.48),  $-1.13363$  (0.48) a.u. In order to produce a singlet scattering state, we choose  $a_1$  to be 1 and  $b_1$  to be  $-1$ .

In Table II, we compare the results for the photoionization cross sections and asymmetry parameters for the various bases. Since we observe very small differences in the eigenphase sums among the four bases, we conclude that the diffuse functions are not essential for the description of the scattering solution. However, the differences between the cross sections for bases 1 and 2 at low energies indicates that such functions should be included in the construction of the target-state wave function. As suggested earlier by O'Neil and Reinhardt,<sup>32</sup> the need for a more diffuse set of basis functions on the target molecule stems from the nature of the dipole matrix element. The integral is not only sensitive to the region around the nuclei, where the tight functions give an adequate representation, but also to the region beyond the nuclei where more diffuse functions are necessary for an accurate representation. The results are in reasonably good agreement with those of other theoretical endeavors,<sup>16(c),16(d),31,32,35</sup> taking into account the different representations for the target, ionic, and continuum wave functions.

### B. Photoionization of $\text{N}_2$

We consider the following two photoionization processes for the ground state of  $\text{N}_2 X^1\Sigma_g^+$ :



The former process is of particular interest due to the existence of a broad shape resonance in the  $\sigma_u$  channel, while the latter process demands special attention owing to the appearance of a spurious  $\pi_{xg}$  shape resonance at the FCHF level.

In Table III we describe the two Gaussian bases used to represent the bound orbitals of  $\text{N}_2$  and  $\text{N}_2^+$  and the orbitals that form the basis of the separable potentials.<sup>36,37</sup>

TABLE I. Gaussian bases for photoionization of ground state  $\text{H}_2$  at  $R_{\text{eq}} = 1.4a_0$ . The conventions are as follows: (1)  $n\gamma/n'\gamma$  implies the contraction of the basis from  $n$  to  $n'$  functions of type  $\gamma$ ; (2)  $n\gamma[X, Y]$  implies that there are  $n$  functions of type  $\gamma$  with the exponent starting with a value of  $X$  and decreasing in increments of  $Y^{-1}$  (geometric progression); (3)  $\gamma$  with no subscript implies that all components are retained (e.g.,  $p$  means that  $p_x, p_y$ , and  $p_z$  are included). The references are to the source of the exponential and contraction coefficients. H refers to the hydrogen nucleus and c.m. to the center of mass.

Center	Basis 1		Basis 2	
	Type	Exponential coefficient	Type	Exponential coefficient
H	$7s/7s$	Ref. 31	$9s$	Ref. 32
	$6p$	Ref. 31	$4p$	Ref. 32
c.m.	$6p_z(\sigma_u)$	[0.02,2]	$6p_z$	[0.02,2]
	$6p_x(\pi_{xu})$		$6p_x$	

TABLE II. Selected values of the eigenphase sums, partial and total photoionization cross sections, and asymmetry parameters for the photoionization of  $H_2$  from  $1\sigma_g$  orbital. The ionization energy is 16.4 eV, and  $k^2$  is the energy of the continuum electron. The scattering parameters are as follows. GTO basis: (1)  $\sigma_u$ ,  $n_c=n_e=6$ ,  $n_f=19$ ; (2)  $\pi_{xu}$ ,  $n_c=n_e=6$ ,  $n_f=10$ . STO bases:  $\sigma_u$ ,  $\pi_u$ ,  $n_c=6$ ,  $n_e=n_b=3$ .  $r_a=r_m=10a_0$ ;  $n_p=37$  [10,15,10|0.7,1.4]. One megabarn (Mb) =  $1.0 \times 10^{-18}$  cm<sup>2</sup>. Only the singlet scattering state is considered. FR refers to the wave function of Fraga and Ransil (Ref. 33) and CW to that of Cade and Wahl (Ref. 34). 1 and 2 refer to the bases in Table I.

$k^2$ (Ry)	$\delta_{\text{sum}}$ (rad)		$\sigma_{\text{ph}}$ (Mb)		$\beta$	
	Method	$\sigma_u$	$\pi_u$	$\sigma_u$		$\pi_u$
0.1838						
	FR	0.2106	-0.2512	4.012	7.184	
	CW	0.2093	-0.2511	4.069	7.178	
	2	0.2084	-0.2482	4.112	7.312	1.922
	1	0.2080		4.483		
0.3362						
	FR	0.2647	-0.2303	2.875	5.782	
	CW	0.2632	-0.2300	2.949	5.812	
	2	0.2626	-0.2291	2.950	5.884	1.915
	1	0.2617		3.139		
1.071						
	FR	0.4301	-0.1493	0.650	2.292	
	CW	0.4291	-0.1486	0.660	2.289	
	2	0.4236	-0.1420	0.630	2.146	1.910
	1	0.4250		0.584		

Both bases have essentially the same form for the nuclear-centered functions with basis 1 having a slightly more extensive diffuse  $s$  and  $p$  set and less tightly bound  $d$  functions. In addition, we include in basis 1 a much more diffuse set of functions at the center of mass in order to give a reasonable degree of flexibility to the separable basis. Basis 1 yields a total energy for  $N_2$  of  $-108.974197$  a.u., while basis 2 gives a value of  $-108.978534$  a.u. The slightly lower result for basis 2 is due primarily to the inclusion of more tightly bound functions, especially in the  $d$  set. Basis 1 gives a quadrupole moment for  $N_2$  of 0.89 a.u. while basis 2 yields a value of 1.02. These results should be compared with the values from the Slater-type basis calculations of Cade *et al.*<sup>38</sup> (0.95) and Nesbet<sup>39</sup> (0.89). That basis 1 gives a better value for the quadrupole moment for  $N_2$  indicates a greater flexibility to represent the outer regions of the bound and separable wave functions. In Table IV, we give

the values of the  $a_i$  and  $b_i$  coefficients for the two scattering cases.

### 1. Photoionization leading to the $X^2\Sigma_g^+$ state of $N_2^+$

In Fig. 1 we compare our total photoionization cross sections for the ionization of the  $3\sigma_g$  orbital of  $N_2$  in the FN, dipole-length approximations for basis 1 with those of the STMT<sup>6</sup> and SV<sup>10</sup> approaches. We obtain very good agreement with the results of the SV method over the entire range of photon energies. The agreement is also reasonable with the STMT method except at low energies. In Fig. 2, we compare our total photoionization cross section with the experimental results of Plummer *et al.*;<sup>40</sup> in addition, we present the partial photoionization cross sections in the  $\sigma_u$  and  $\pi_{xu}$  scattering channels. The FCHF values are somewhat too high at the position of the resonance ( $\sim 29$  eV) and too low for small photon energies.

TABLE III. Gaussian bases for photoionization of the ground state of  $N_2$  at  $R_{\text{eq}}=2.068a_0$ . Conventions as described in Table I.

Center	Basis 1		Basis 2	
	Type	Exponential coefficient	Type	Exponential coefficient
N	9s/5s	Ref. 36	9s/4s	Ref. 36
	1s	0.06	6s	[16,2]
	5p/3p	Ref. 36	5p/3p	Ref. 37
	1p	0.05	2p	[1,2]
	2d	0.98,0.16	2d	1.58,0.47
c.m.	$6p_z(\sigma_u)$	[0.025,2]	$4p_z(\sigma_u)$	[4,2]
	$6p_x(\pi_{xu})$	[0.025,2]		

TABLE IV. Coefficients  $a_i$  and  $b_i$  for the Coulomb and exchange operators [Eq. (22)] for electron scattering from  $N_2^+$ . The core  $c$  refers to the  $1\sigma_g$ ,  $2\sigma_g$ ,  $1\sigma_u$ , and  $2\sigma_u$  orbitals.

Ionized orbital	Scattering symmetries	$c$	$(a_i, b_i)$		
			$3\sigma_g$	$1\pi_x$	$1\pi_y$
$3\sigma_g$	$k\sigma_u, k\pi_{xu}$	(1,1)	(1, -1)	(1,1)	(1,1)
$1\pi_{xu}$	$k\pi_{xg}, \pi_{xg}$	(1,1)	(1,1)	$(\frac{1}{4}, -3)$	$(\frac{5}{4}, 5)$

Lucchese *et al.*<sup>10</sup> have shown that better agreement with experiment can be obtained in both energy regimes by using a CI target wave function. Still, the FCHF results are within 30% of experiment over most of the energy range, and the major features are faithfully reproduced. In Table V we present selected results for the eigenphase sums, the partial and total photoionization cross sections, and the asymmetry parameter calculated with basis 1.

While the agreement between the dipole-length LA and SV results are quite encouraging, there remain some small differences of the order of 10–20% in the region below the resonance peak ( $E_{ph} \leq 29$  eV). At very low photon energies, the SV results are lower than the LA ones, while at intermediate energies (20–25 eV), the trend is reversed. Most of the difference can be ascribed to the choice of target wave function. In Table VI, we present a comparison of eigenphase sums and photoionization cross sections for the  $\sigma_u$  channel employing different forms of the target and continuum wave functions. For this exercise, we build on basis 2, which is quite similar to that of Lucchese *et al.*<sup>10</sup> In case (1) we represent the  $N_2$ ,  $N_2^+$ , and separable exchange orbitals by basis 2. For case (2) we add a set of diffuse functions at the c.m. for the separable orbitals and leave the bound  $N_2$  and  $N_2^+$  orbitals in terms of basis 2. Finally, in case (3) we represent all orbitals in the augmented basis 2. In all cases, the eigenphase sums change very little, indicating that the diffuse functions are not necessary for an accurate description of the continuum orbital. This observation is reinforced by noting the comparatively small change effected in the photoioniza-

tion cross section by going from case (1) to (2). However, the fact that the photoionization cross section at the lower photon energies changes by as much as 10% between cases (2) and (3) indicates that diffuse functions are important in describing the *target* wave function. This is similar to the conclusion we drew from the photoionization of  $H_2$ . We have simply reinforced it here and demonstrated that it is also valid for larger molecular systems. Similar differences arise in the  $\pi_u$  channel leading to total photoionization cross sections differing by 10–20%.

## 2. Photoionization leading to the $A^2\Pi_u$ state of $N_2^+$

As a demonstration of our techniques for the photoionization of the  $1\pi_u$  orbital, we consider only  $k\pi_{xg}$  scattering. Since we employ Cartesian Gaussians in the description of the various wave functions, the  $J$  and  $K$  operators are noncylindrical for scattering in the  $\pi_g$  channel. Thus this channel provides an opportunity to test the LA routines for this more general case. In Fig. 3, we present the partial photoionization cross section for ionization of the  $1\pi_u$  orbital of  $N_2$  in the dipole-length and FCHF approximations. We notice the appearance of a strong resonance at low photon energies in agreement with the earlier STMT<sup>6</sup> and SV calculations.<sup>10</sup> This resonance, however, is known to be spurious.<sup>6,10</sup> The HF potential improperly places an excited  $\pi$  state above the ionization limit. When proper account is taken of  $\sigma$  correlations and  $\sigma$ - $\pi$  coupling, this feature moves below the ionization threshold. The resonance feature disappears, and the photoionization

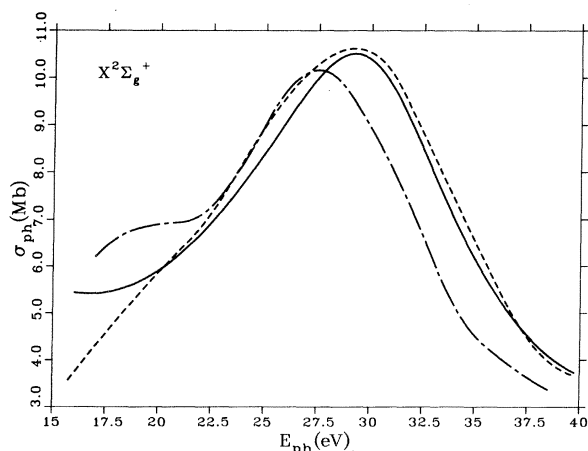


FIG. 1. Total cross sections for the photoionization of  $N_2$  leading to the  $X^2\Sigma_g^+$  state of  $N_2^+(3\sigma_g^{-1})$ . Comparison of theoretical methods: solid line, LA; dashed line, SV, Ref. 10; chain-dashed line, STMT, Ref. 6.

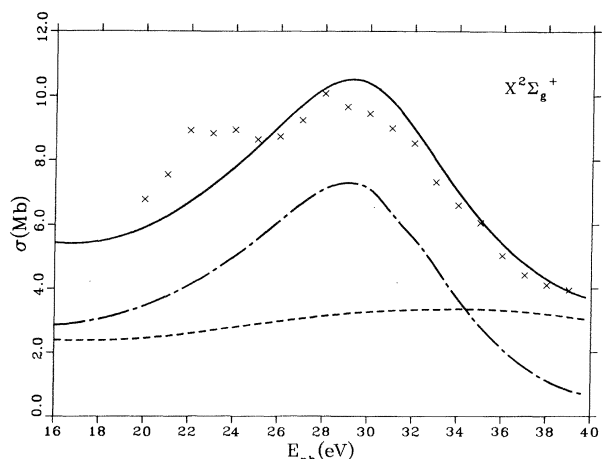


FIG. 2. Partial and total cross sections for the photoionization of  $N_2$  ( $N_2^+ X^2\Sigma_g^+$ ). Comparison of the LA method and experiment: solid line, total; chain-dashed line,  $3\sigma_g \rightarrow k\sigma_u$ ; dashed line  $3\sigma_g \rightarrow k\pi_u$ ; crosses, expt. (Ref. 40).



TABLE V. Selected values of the eigenphase sums, partial and total photonization cross sections, and the asymmetry parameter for the photoionization of  $N_2$  from the  $3\sigma_g$  orbital in basis 1 leading to the  $^2\Sigma_g^+$  state of  $N_2^+$ . The ionization energy is 15.6 eV. The parameters for the scattering calculation are as follows: (1)  $\sigma_u$ ,  $n_c=n_e=16$ ,  $n_f=18$ ; (2)  $\pi_{xu}$ ,  $n_c=n_e=10$ ,  $n_f=12$ ;  $r_a=r_m=10a_0$ ,  $n_p=100$  [15,40,25,20|0.7,1.5,2.5].

$E_{ph}$ (eV)	$\delta_{sum}$ (rad)		$\sigma_{ph}$ (Mb)		Total	$\beta$
	$\sigma_u$	$\pi_u$	$\sigma_u$	$\pi_u$		
16.0	1.810	2.108	2.855	2.592	5.447	1.644
20.0	1.613	2.024	3.464	2.446	5.909	1.142
25.0	1.600	1.974	5.520	2.881	8.402	1.027
27.0	1.708	1.959	6.653	3.064	9.717	0.995
29.0	1.903	1.952	7.293	3.211	10.504	0.942
31.0	2.162	1.957	6.354	3.307	9.847	0.868
35.0	2.621	2.007	2.828	3.317	6.145	0.724
40.0	2.908	2.128	0.670	3.012	3.681	0.693

TABLE VI. Comparison of different constructions of the target and scattering bases for photoionization of  $N_2$  out of the  $3\sigma_g$  orbital and scattering in the  $\sigma_u$  symmetry. Cases presented: (1) basis 2 for the target and continuum; (2) basis 2 for the target, basis 2 + diffuse c.m. set of basis 1 for continuum; (3) basis 2 + diffuse set for target and continuum. The scattering parameters for the  $\sigma_u$  symmetry are the same as in Table V.

$E_{ph}$ (eV)	$\delta_{sum}$ (rad)			$\sigma_{ph}$ (Mb)		
	(1)	(2)	(3)	(1)	(2)	(3)
16.0	1.792	1.794	1.794	2.704	2.684	2.996
25.0	1.656	1.662	1.662	6.129	6.155	5.665
28.0	1.838	1.835	1.835	7.179	7.200	6.846
30.0	2.045	2.043	2.043	6.929	7.009	6.825
32.5	2.354	2.363	2.363	4.993	5.045	5.063

TABLE VII. Gaussian basis for photoionization of ground state NO at  $R_{eq}=2.175a_0$ . Conventions are the same as in Table I.

Center	Type	Exponential coefficients
N	9s/5s	Ref. 36
	1s	0.05
	6p/3p	Ref. 36
	1p	0.05
	2d	0.98,0.16
O	9s/5s	Ref. 36
	1s	0.05
	6p/3p	Ref. 36
	1p	0.05
	2d	0.80,0.15
c.m.	4p <sub>x</sub> ( $\pi_{xu}$ )	[0.025,2]
	5d <sub>xz</sub>	[0.05,2]

TABLE VIII. Selected values of the partial and total photoionization cross section and asymmetry parameter for photoionization of NO from the  $2\pi$  orbital leading to the  $X^1\Sigma^+$  state of  $NO^+$ . The ionization potential is 9.26 eV. The scattering parameters are as follows: (1)  $\sigma$ ,  $n_c=n_e=21$ ,  $n_f=35$ ; (2)  $\pi_x$ ,  $n_c=n_e=12$ ,  $n_f=21$ ; (3)  $\delta_{xy}$ ,  $n_c=n_e=11$ ,  $n_f=9$ ;  $r_a=r_m=10a_0$ ,  $n_p=56$  [7,23,12,14|0.7,1.5,2.5]. Scattering takes place in the doublet spin state.

$E_{ph}$ (eV)	$\sigma_{ph}$ (Mb)			Total	$\beta$
	$\sigma$	$\pi$	$\delta$		
10.0	0.437	0.458	0.511	1.406	-0.214
12.0	0.896	0.797	0.833	2.526	0.090
14.0	1.509	1.099	1.068	3.676	0.179
16.0	0.714	1.333	1.222	3.269	0.149
20.0	0.338	1.733	1.398	3.469	0.533
24.0	0.287	2.069	1.459	3.815	0.794
28.0	0.261	2.113	1.460	3.834	0.969
32.0	0.227	1.752	1.396	3.375	1.076
36.0	0.191	1.263	1.279	2.733	1.139
40.0	0.163	0.881	1.145	2.189	1.186

TABLE IX. Gaussian bases for photoionization of ground state CO<sub>2</sub> at  $R_{C-O}=2.1944a_0$ . Conventions as in Table I, where not mentioned, type and coefficient are the same as basis 1.

Center	Basis 1		Basis 2		Basis 3	
	Type	Exponential coefficient	Type	Exponential coefficient	Type	Exponential coefficient
O	9s/5s	Ref. 36			9s/5s	Ref. 36
	5p/3p	Ref. 36			5p/4p	Ref. 36
	1p	0.05			1p	0.05
	1d	0.85			2d	0.85,0.15
C	9s/5s	Ref. 36			9s/5s	Ref. 36
	5p/3p	Ref. 36	5p/5p	Ref. 36	5p/5p	Ref. 36
	1p	0.05			1p	0.05
	1d	0.75			1d	0.75
c.m.	6p <sub>z</sub> (σ <sub>u</sub> )	[0.025,2]				
	6p <sub>x</sub> (π <sub>xu</sub> )	[0.025,2]				

TABLE X. Convergence study: CO<sub>2</sub><sup>+</sup>(4σ<sub>g</sub><sup>-1</sup>)+kσ<sub>u</sub> in the FCHF approximation. The parameters are as follows: n<sub>e</sub>=18, n<sub>f</sub>=23, basis 2, r<sub>a</sub>=r<sub>m</sub>=10a<sub>0</sub> [10,14,20,10,5|0.5,1.9,2.5,4]. k<sup>2</sup>=E<sub>ph</sub>-IP.

k <sup>2</sup> (Ry)	δ <sub>sum</sub> (rad)			
	n <sub>c</sub> =18	n <sub>c</sub> =22	n <sub>c</sub> =26	n <sub>c</sub> =30
1.147	0.682	0.734	0.772	0.784
1.514	0.814	0.930	1.020	1.049
1.588	0.997	1.159	1.282	1.321
1.882	2.401	2.503	2.560	2.577

σ <sub>ph</sub> (Mb)				
1.147	3.299	3.398	3.474	3.498
1.514	5.341	5.722	6.049	6.132
1.588	6.385	6.763	6.875	6.884
1.882	0.878	0.628	0.525	0.499

TABLE XI. Selected values of the eigenphase sums, partial and total photoionization cross sections, and asymmetry parameter for photoionization of CO<sub>2</sub> from the 4σ<sub>g</sub> orbital leading to the C<sup>2</sup>Σ<sub>g</sub><sup>+</sup> state of CO<sub>2</sub><sup>+</sup>. The ionization energy is 19.4 eV. The parameters for the scattering calculation are as follows: (1) σ<sub>u</sub>, n<sub>c</sub>=30, n<sub>e</sub>=18, n<sub>f</sub>=23 (basis 2); (2) π<sub>u</sub>, n<sub>c</sub>=n<sub>e</sub>=14, n<sub>f</sub>=15 (basis 1); r<sub>a</sub>=r<sub>m</sub>=10a<sub>0</sub>, n<sub>p</sub>=59 [10,14,20,10,5|0.5,1.9,2.5,4]. Scattering takes place in the singlet spin state.

E <sub>ph</sub> (eV)	δ <sub>sum</sub> (rad)		σ <sub>ph</sub> (Mb)		Total	β
	σ <sub>u</sub>	π <sub>xu</sub>	σ <sub>u</sub>	π <sub>u</sub>		
25.0	1.201	1.478	2.183	0.462	2.645	1.441
30.0	0.950	1.237	2.876	0.742	3.618	1.596
35.0	0.784	1.036	3.506	1.023	4.529	1.561
40.0	1.049	0.932	6.161	1.242	7.403	1.107
41.0	1.321	0.921	6.992	1.272	8.194	0.848
41.5	1.510	0.916	6.709	1.285	7.994	0.684
42.0	1.726	0.911	5.876	1.296	7.172	0.498
43.0	2.138	0.903	3.135	1.316	4.441	0.146
44.0	2.416	0.895	1.263	1.331	2.594	0.045
45.0	2.577	0.888	0.503	1.341	1.844	0.299

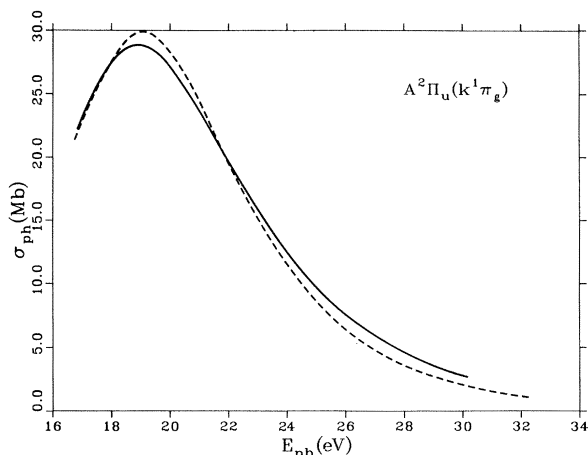


FIG. 3. Partial cross sections for the photoionization of  $N_2$  leading to the  $A^2\Pi_u$  state of  $N_2^+(1\pi_u^{-1})$ . Comparison of theoretical methods for  $1\pi_u \rightarrow k\pi_g$ : solid line, LA; dashed line, SV (Ref. 10).

cross section agrees much better with experiment.

Several prescriptions have been proposed and implemented for obtaining a more physical result by directly modifying the HF potential.<sup>10</sup> The optical potential formulation should also lead to the desired results since the proper excited-state correlations and couplings are included in  $V_{opt}$ . Unfortunately, its present restriction to a single, open scattering channel does not allow an application to be made to this case since the use of Cartesian Gaussians forces a formulation in terms of two coupled, degenerate channels. We are currently developing a set of programs to handle sets of coupled, open electronic channels.

### C. Photoionization of NO

We consider the following photoionization process for NO in the ground  $X^2\Pi$  state:

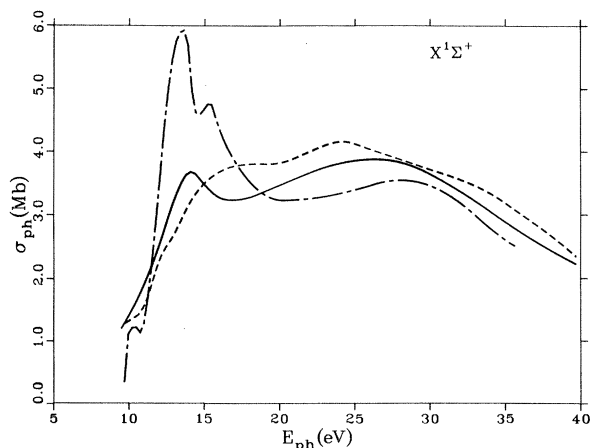


FIG. 4. Total cross section for the photoionization of NO leading to the  $X^1\Sigma^+$  state of  $NO^+(2\pi^{-1})$ . Comparison of theoretical methods: solid line, LA; dashed line, SV (Ref. 11); chain-dashed line STMT (Ref. 7).

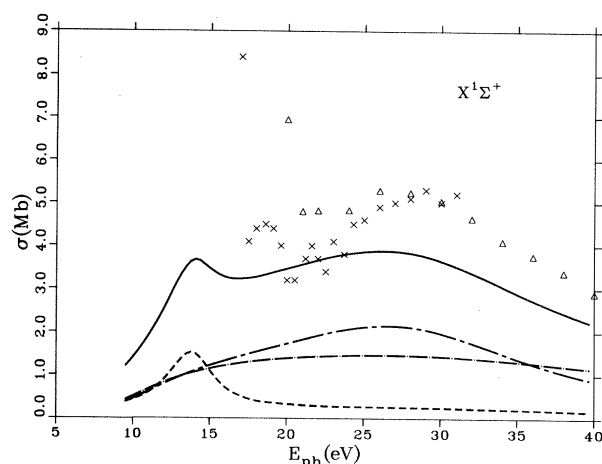
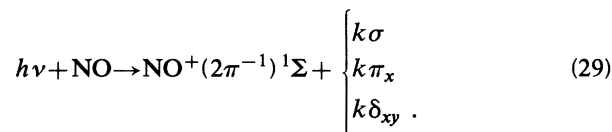


FIG. 5. Partial and total cross sections for the photoionization of NO ( $NO^+ X^1\Sigma^+$ ). Comparison of the LA method and experiment: solid line, total; chain-dashed line,  $2\pi \rightarrow k\pi$ ; dashed line,  $2\pi \rightarrow \sigma$ ; dotted line,  $2\pi \rightarrow k\delta$ ; crosses, expt. (Ref. 42); triangles, expt. (Ref. 41).



Our interest in this process stems from a desire to resolve the rather large differences between the Stieltjes and Schwinger results. In Table VII we present the basic parameters for the Gaussian basis used to describe NO. The basis produces a total energy of  $-129.268$  a.u. for NO and a dipole moment of 0.65 a.u. for  $NO^+$ . Since we are scattering from a closed-shell ion, the coefficients  $a_i$  and  $b_i$  are 1 for all orbitals.

In Fig. 4 we compare our total photoionization cross sections with those of the STMT<sup>7</sup> and SV<sup>11</sup> methods. Our results are in very good agreement with those of the Schwinger variational method. We observe no structure in the individual partial photoionization cross sections as

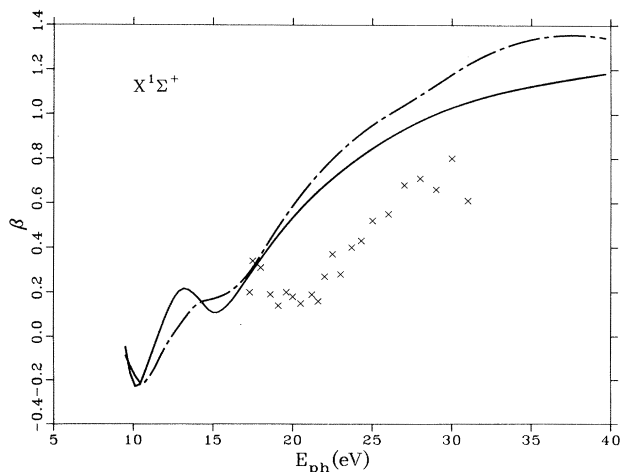


FIG. 6. Asymmetry parameter (ITAD) for photoionization of NO ( $NO^+ X^1\Sigma^+$ ). Comparison of theoretical and experimental results: solid line, LA; chain-dashed line, SV (Ref. 11); crosses, expt. (Ref. 44).

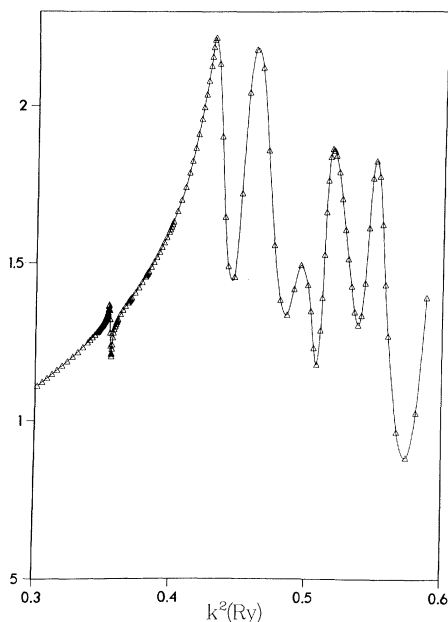


FIG. 7. Partial cross sections for the photoionization of NO ( $\text{NO}^+ X^1\Sigma^+$ ) calculated with the effective-optical-potential approach ( $2\pi \rightarrow k\pi$ ). Abscissa is labeled by photoelectron energy  $k^2$  in Ry [ $E_{\text{ph}}(\text{eV}) = 13.6k^2 + 9.26$ ].

is apparent from Fig. 5 where we also compare to the results of the  $(e,2e)$  experiment of Brion and Tan<sup>41</sup> and the synchrotron experiment of Southworth *et al.*<sup>42</sup> In Fig. 6 we compare our  $\beta$  parameter with that of the SV method.<sup>11</sup> Small differences are noted at low photon energies due to the slightly different positions of the  $\sigma$  resonance. The difference can, as with  $\text{N}_2$ , be ascribed to the choice of the basis. The effect in NO is somewhat more pronounced since the resonance feature is sharper. We present selected values of the eigenphase sums, partial and total photoionization cross sections, and the asymmetry parameters for photoionization of the  $2\pi$  orbital for NO in Table VIII. Finally, in Fig. 7, we present the photoion-

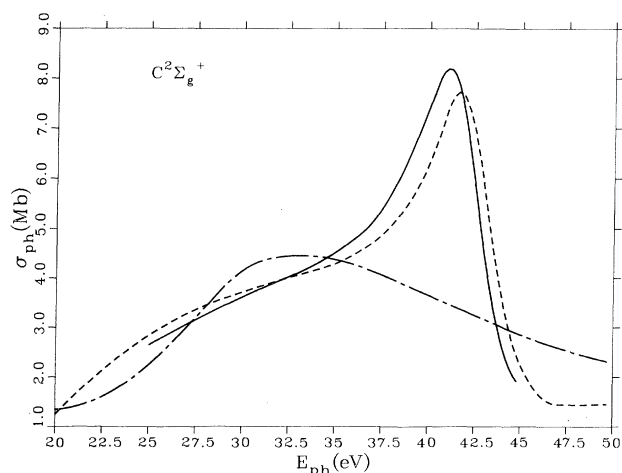
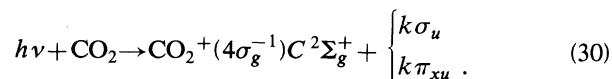


FIG. 8. Total cross sections for the photoionization of  $\text{CO}_2$  leading to the  $\text{C}^2\Sigma_g^+$  state of  $\text{CO}_2(4\sigma_g^-)$ . Comparison of theoretical methods: solid line, LA; dashed line, SV (Ref. 12); chain-dashed line, STMT (Ref. 8).

ization cross section for the  $\pi_x$  channel in the case that the continuum solution is determined by the effective optical-potential approach. This calculation was performed with a limited basis and only meant to demonstrate the validity of such an approach. Still, it is gratifying to note the appearance of autoionization features.

#### D. Photoionization of $\text{CO}_2$

We consider the following process for photoionization of the ground  $X^1\Sigma_g^+$  state of  $\text{CO}_2$ :



We are particularly interested in this process since, as with NO, there are considerable differences between the predictions of the Stieltjes and Schwinger methods. The Schwinger method<sup>12</sup> predicts a narrow shape resonance at about 41 eV in the  $\sigma_u$  channel while the Stieltjes<sup>8</sup> calculations show no such feature.

In Table IX we describe three bases employed to represent the  $\text{CO}_2$ ,  $\text{CO}_2^+$ , and separable exchange orbitals. For neutral  $\text{CO}_2$ , the total energies (quadrupole moment) are  $-187.6719$  (4.5),  $-187.6720$  (4.26), and  $-187.6754$  (3.78) a.u. for bases 1, 2, and 3, respectively. The experimental value for the quadrupole moment is 3.20 a.u.<sup>43</sup> The  $a_i$  and  $b_i$  coefficients for the core orbitals are, as usual, (1,1), while for the  $3\sigma_g$  orbital they are 1 and  $-1$ , respectively. This choice produces a singlet scattering state.

Before proceeding to a presentation of the results, we first demonstrate the efficacy of the single-center expansion and CC approximation for representing the  $\sigma_u$  scattering wave function. This symmetry provides the most strenuous test of this prescription since 30 channels are required to converge the various scattering and photoionization quantities. In Table X we present a detailed compilation of the results of our convergence study with basis 2. We follow the eigenphase sum and partial photoionization cross section as a function of the number of expansion terms  $n_c$  retained in Eq. (14a). This choice translates into the solution of a set of coupled integral equations of order  $n_c$ . We note that the choice  $n_c = 30$  produces quantities converged to within 5% or better. We have also tested the convergence with respect to the choice of  $n_e$ ,  $r_a$ ,  $r_m$ , and  $n_f$  and found similarly small sensitivities. These convergence parameters are quite close to those found by Lucchese and McKoy<sup>12</sup> with the Schwinger method. We have also performed  $\sigma_u$  calculations in all three bases. We observe very little sensitivity to the nature of the basis whether more diffuse or less contracted.

In Fig. 8 we compare our total photoionization cross section with those of the SV<sup>12</sup> and STMT<sup>8</sup> methods in the dipole-length and FCHF approximation. We note that our results follow quite closely those of the Schwinger method.<sup>12</sup> The  $\sigma_u$  resonant feature is quite apparent in both calculations at about 41 eV. On the other hand, the STMT shows no feature in this energy regime. As with  $\text{N}_2$  and NO, there are slight differences between the results of the LA and SV calculations. We find the peak

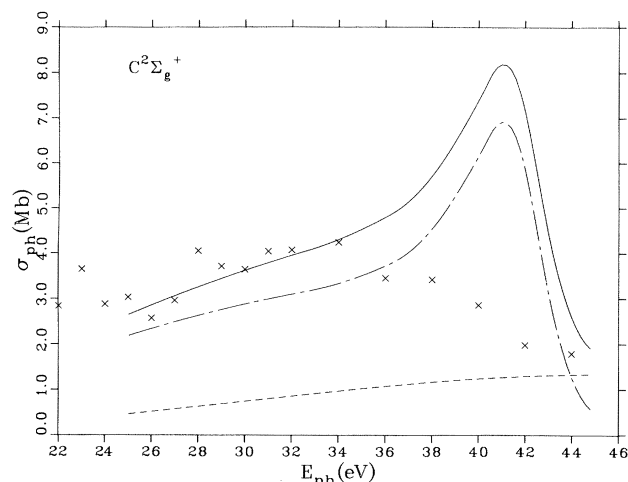


FIG. 9. Partial and total cross sections for the photoionization of  $\text{CO}_2$  ( $\text{CO}_2^+ C^2\Sigma_g^+$ ). Comparison of the LA method with experiment: solid line, total; chain-dashed line,  $4\sigma_g \rightarrow k\sigma_u$ ; dashed line,  $4\sigma_g \rightarrow k\pi_u$ ; crosses, expt. (Ref. 44).

position to be about 41.25 eV while the SV<sup>12</sup> method returns a result nearer to 41.8 eV. We believe that these differences can be attributed to the slightly different basis sets employed and not to any inherent problems with either calculation or method. In Fig. 9, we also compare our total photoionization cross section with the experimental results of Tan and Brion.<sup>44</sup> We note that the experimental results show no evidence of a resonance. However, Lucchese and McKoy<sup>12</sup> have shown that the sharp resonant peak near 41 eV is damped by the introduction of correlation into the target wave function and of vibrational effects. Therefore, the final verdict is not yet in. However, the comparison with experiment is somewhat of a side issue, since in the FCHF and dipole-length approximations all three methods should give the same results. We present a summary of our results in Table XI. Finally, in Fig. 10, we give a comparison of our  $\beta$  parameters with that of Lucchese and McKoy.<sup>12</sup> Again, taking into account the slight shift in the resonance position due to a different choice of basis, the results are in quite good agreement.

#### IV. SUMMARY

We have extended our linear algebraic method for calculating electron-molecule scattering information to photoionization processes. We have performed calculations at the fixed-nuclei frozen-core, Hartree-Fock level for the photoionization of ground state  $\text{H}_2$ ,  $\text{N}_2$ ,  $\text{NO}$ , and  $\text{CO}_2$ . We obtained very good agreement in all four cases with

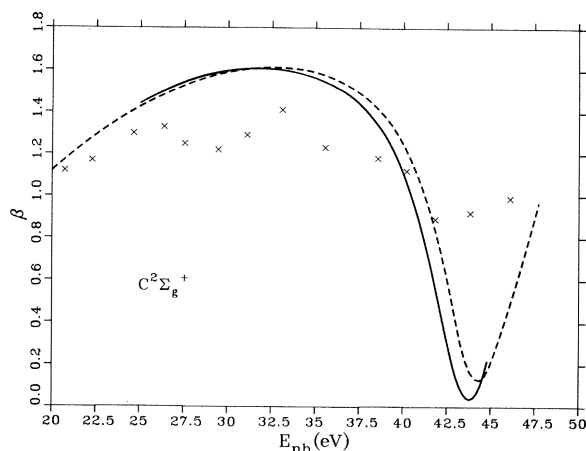


FIG. 10. Asymmetry parameter (ITAD) for the photoionization of  $\text{CO}_2$  ( $\text{CO}_2^+ C^2\Sigma_g^+$ ). Comparison of theoretical and experimental results: solid line, LA; dashed line, SV (Ref. 12); crosses, expt. (Ref. 45).

the Schwinger variational results of McKoy and co-workers. For  $\text{N}_2$  our calculations agree reasonably well with those of the STMT; however, for  $\text{NO}$  and  $\text{CO}_2$  we obtain rather different results. We do not reproduce any of the structure in the total and partial photoionization cross sections for ionizing the  $2\pi$  orbital of  $\text{NO}$  that is reported from the STMT calculations. Also, for the ionization of the  $4\sigma_g$  orbital of  $\text{CO}_2$ , we obtain a sharp shape resonance in the  $\sigma_u$  channel which does not appear in the STMT results. In addition, we have introduced correlation effects into the elastic scattering channel through an effective optical potential and obtained autoionizing features for  $\text{NO}$  photoionization.

#### ACKNOWLEDGMENTS

We wish to acknowledge useful conversations with Dr. A. Hazi, Dr. T. Rescigno, and Dr. R. Martin. We especially wish to thank Professor V. McKoy for useful suggestions regarding the general implementation of the photoionization formalism and, in particular, the convergence problems associated with the  $\text{CO}_2$  system and for providing us with tabular representations of the figures in some of his papers. We also wish to thank Dr. Z. Levine for providing us with tables of the experimental  $\text{N}_2$  results. This work was performed under the auspices of the U. S. Department of Energy through the Theoretical Division of the Los Alamos National Laboratory.

<sup>1</sup>J. Berkowitz, *Photoabsorption, Photoionization, and Photoelectron Spectroscopy* (Academic, New York, 1979); J. A. R. Samson, in *Electronic Spectroscopy: Theory, Techniques and Applications*, edited by C. R. Brundle and A. D. Baker (Academic, London, 1981), Vol. 4, p. 361.

<sup>2</sup>(a) J. B. Polluck and Y. L. Yung, *Annu. Rev. Earth Planet. Sci.* **8**, 407 (1980); G. E. Hunt, *ibid.* **11**, 415 (1983); (b) W. F.

Huebner, P. T. Giguere, and W. L. Slattery, in *Comets*, edited by L. L. Wilkening (University of Arizona, Tucson, 1982); W. D. Watson, *Ann. Rev. Astron. Astrophys.* **16**, 585 (1978).

<sup>3</sup>E. W. Plummer and W. Eberhardt, *Adv. Chem. Phys.* (to be published); A. Bienenstock and H. Winick, *Physics Today* **36**, 48 (1983).

<sup>4</sup>M. O. Krause, in *Synchrotron Radiation Research*, edited by S.

- Doniach and H. Winick (Plenum, New York, 1980).
- <sup>5</sup>P. W. Langhoff, *Electron-Atom and Electron-Molecule Collisions*, edited by J. Hinze (Plenum, New York, 1983), p. 297.
- <sup>6</sup>T. N. Rescigno, C. F. Bender, V. McKoy, and P. W. Langhoff, *J. Chem. Phys.* **68**, 970 (1978); T. N. Rescigno, A. Gerwer, V. McKoy, and P. W. Langhoff, *Chem. Phys. Lett.* **78**, 21 (1981).
- <sup>7</sup>J. J. Delaney, I. H. Hillier, and V. R. Sanders, *J. Phys. B* **15**, 1474 (1982).
- <sup>8</sup>N. T. Padial, G. Csanak, V. McKoy, and P. W. Langhoff, *J. Chem. Phys.* **69**, 2992 (1978).
- <sup>9</sup>D. K. Watson and V. McKoy, *Phys. Rev. A* **20**, 1474 (1979); R. R. Lucchese and V. McKoy, *ibid.* **21**, 112 (1980); **24**, 770 (1981).
- <sup>10</sup>R. R. Lucchese, G. Raseev, and V. McKoy, *Phys. Rev. A* **25**, 2572 (1982).
- <sup>11</sup>M. E. Smith, R. R. Lucchese, and V. McKoy, *J. Chem. Phys.* **79**, 1360 (1983).
- <sup>12</sup>R. R. Lucchese and V. McKoy, *Phys. Rev. A* **26**, 1406 (1982).
- <sup>13</sup>(a) D. Dill and J. L. Dehmer, *J. Chem. Phys.* **61**, 692 (1974); **65**, 5327 (1977); J. A. Stephens, D. Dill, and J. C. Dehmer, *J. Phys. B* **14**, 3911 (1981); P. M. DiHerman, D. Dill, and J. L. Dehmer, *J. Chem. Phys.* **76**, 5703 (1982); (b) J. R. Swanson, D. Dill, and J. L. Dehmer, *J. Phys. B* **14**, L207 (1981); (c) S. Wallace, D. Dill, and J. L. Dehmer, *J. Chem. Phys.* **76**, 1217 (1981).
- <sup>14</sup>H. P. Kelly, *Chem. Phys. Lett.* **20**, 547 (1973); T. E. H. Walker and H. P. Kelly, *ibid.* **16**, 511 (1972).
- <sup>15</sup>(a) Z. H. Levine and P. Soven, *Phys. Rev. Lett.* **50**, 2074 (1983); (b) G. R. J. Williams and P. W. Langhoff, *Chem. Phys. Lett.* **78**, 21 (1981).
- <sup>16</sup>(a) G. Raseev, H. Le Rouzo, and H. Lefebvre-Brion, *J. Chem. Phys.* **72**, 5701 (1980); (b) W. D. Robb and L. A. Collins, *Phys. Rev. A* **22**, 2474 (1980); (c) C. M. Dutta, F. M. Chapman, and E. F. Hayes, *J. Chem. Phys.* **67**, 1904 (1977); (d) Y. Itikawa, H. Takagi, H. Nakamura, and H. Sato, *Phys. Rev. A* **27**, 1319 (1983).
- <sup>17</sup>L. A. Collins and B. I. Schneider, *Phys. Rev. A* **24**, 2387 (1981); B. I. Schneider and L. A. Collins, *ibid.* **24**, 1264 (1981).
- <sup>18</sup>B. I. Schneider and L. A. Collins, *Phys. Rev. A* **21**, 2847 (1983); **28**, 166 (1983).
- <sup>19</sup>L. A. Collins and B. I. Schneider, *Phys. Rev. A* **27**, 101 (1983).
- <sup>20</sup>J. C. Tully, R. S. Berry, and B. J. Dalton, *Phys. Rev.* **176**, 95 (1968); B. I. Schneider and R. S. Berry, *ibid.* **182**, 141 (1969).
- <sup>21</sup>A. Temkin and K. V. Vasavada, *Phys. Rev.* **160**, 109 (1967).
- <sup>22</sup>D. Dill, *Phys. Rev. A* **7**, 1976 (1973).
- <sup>23</sup>(a) *Methods of Electronic Structure Theory*, edited by H. F. Schaefer III (Plenum, New York, 1977); (b) *Algorithms and Computer Codes for Atomic and Molecular Quantum Scattering Theory*, edited by L. Thomas (University of California, Berkeley, 1979).
- <sup>24</sup>H. Feshbach, *Ann. Phys. (N.Y.)* **5**, 357 (1958).
- <sup>25</sup>J. B. Rose and V. McKoy, *J. Chem. Phys.* **55**, 5435 (1971).
- <sup>26</sup>B. I. Schneider, *Phys. Rev. A* **7**, 557 (1973).
- <sup>27</sup>J. C. Light and R. B. Walker, *J. Chem. Phys.* **65**, 4272 (1976); B. I. Schneider and R. B. Walker, *ibid.* **70**, 2466 (1979).
- <sup>28</sup>T. N. Rescigno and A. E. Orel, *Phys. Rev. A* **24**, 1267 (1981).
- <sup>29</sup>M. A. Morrison and L. A. Collins, *Phys. Rev. A* **17**, 918 (1978); M. A. Morrison, in *Electron-Molecule and Photon-Molecule Collision*, edited by T. Rescigno, V. McKoy, and B. Schneider (Plenum, New York, 1979), p. 15.
- <sup>30</sup>L. A. Collins, W. D. Robb, and M. A. Morrison, *Phys. Rev. A* **21**, 488 (1980); M. A. Morrison, N. F. Lane, and L. A. Collins, *ibid.* **15**, 2186 (1977); L. A. Collins and D. W. Norcross, *ibid.* **18**, 467 (1978); B. D. Buckley and P. G. Burke, *J. Phys. B* **10**, 725 (1977); M. A. Crees and D. L. Moores, *ibid.* **8**, L195 (1975); N. T. Padial, D. W. Norcross, and L. A. Collins, *Phys. Rev. A* **27**, 141 (1983).
- <sup>31</sup>R. R. Lucchese and V. McKoy, *Phys. Rev. A* **24**, 770 (1981).
- <sup>32</sup>S. V. O'Neil and W. P. Reinhardt, *J. Chem. Phys.* **69**, 2126 (1978).
- <sup>33</sup>S. Fraga and B. J. Ransil, *J. Chem. Phys.* **35**, 1967 (1961).
- <sup>34</sup>P. E. Cade and A. C. Wahl, *At. Data Nucl. Data Tables* **13**, 339 (1974).
- <sup>35</sup>B. Ritchie and B. R. Tambe, *J. Chem. Phys.* **68**, 755 (1978).
- <sup>36</sup>T. H. Dunning and P. J. Hay, in *Methods of Electronic Structure Theory*, edited by H. F. Schaefer III (Plenum, New York, 1977), p. 1.
- <sup>37</sup>T. H. Dunning, *J. Chem. Phys.* **53**, 2823 (1970).
- <sup>38</sup>P. E. Cade, K. D. Sales, and A. C. Wahl, *J. Chem. Phys.* **44**, 1973 (1966).
- <sup>39</sup>R. K. Nesbet, *J. Chem. Phys.* **40**, 3619 (1964).
- <sup>40</sup>E. W. Plummer, T. Gustafsson, W. Gudat, and D. E. Eastman, *Phys. Rev. A* **15**, 2339 (1977).
- <sup>41</sup>C. E. Brion and K. H. Tan, *Electron Spectrosc. Relat. Phenom.* **23**, 1 (1983).
- <sup>42</sup>S. Southworth, C. M. Truesdale, P. H. Kobin, D. W. Linde, W. D. Brewer, and D. A. Shirely, *J. Chem. Phys.* **76**, 143 (1982).
- <sup>43</sup>A. D. Buckingham, R. L. Disch, and D. A. Danner, *J. Am. Chem. Soc.* **90**, 3104 (1968).
- <sup>44</sup>C. E. Brion and K. H. Tan, *Chem. Phys.* **34**, 141 (1978).
- <sup>45</sup>T. A. Carsen, M. O. Krause, F. A. Grimm, J. D. Allen, Jr., D. Mehaffy, P. R. Keller, and J. W. Taylor, *Phys. Rev. A* **23**, 3316 (1981).